Plant Physiology®

The rice phosphate transporter OsPHT1;7 plays a dual role in phosphorus redistribution and anther development

Changrong Dai,[1] Xiaoli Dai,[1,2,3] Hongye Qu,[1,2,3] Qin Men,[1] Jingyang Liu,[1] Ling Yu (ORCID) ,[1,2,3] Mian Gu (ORCID) ,[1,2,3,*,†] and Guohua Xu (ORCID) [1,2,3]

1 State Key Laboratory of Crop Genetics and Germplasm Enhancement, Nanjing Agricultural University, Nanjing 210095, China
2 MOA Key Laboratory of Plant Nutrition and Fertilization in Lower-Middle Reaches of the Yangtze River, Nanjing 210095, China
3 Jiangsu Collaborative Innovation Center for Solid Organic Waste Resource Utilization, Nanjing, 210095 China

*Author for correspondence: gum@njau.edu.cn
†Senior author

M.G. conceived and designed the experiments. C.R.D. performed most of the experiments, and M.G. conducted the immunostaining and anatomic analysis. X.L.D. and H.Y.Q. performed hydroponic culture and rice transformation. Q.M. and J.Y.L. were responsible for the field management and assisted in the physiological analysis. C.R.D. and M.G. analyzed the data, and wrote the article. L.Y. and G.H.X. gave critical comments and revisions to the manuscript.

The author responsible for distribution of materials integral to the findings presented in this article in accordance with the policy described in the Instructions for Authors (https://academic.oup.com/plphys/pages/general-instructions) is Mian Gu (gum@njau.edu.cn).

Abstract

Inorganic phosphate (Pi) is the predominant form of phosphorus (P) readily accessible to plants, and *Pi Transporter 1* (*PHT1*) genes are the major contributors to root Pi uptake. However, the mechanisms underlying the transport and recycling of Pi within plants, which are vital for optimizing P use efficiency, remain elusive. Here, we characterized a functionally unknown rice (*Oryza sativa*) PHT1 member barely expressed in roots, *OsPHT1;7*. Yeast complementation and *Xenopus laevis* oocyte assay demonstrated that OsPHT1;7 could mediate Pi transport. Reverse-transcription quantitative polymerase chain reaction and histochemical analyses showed that *OsPHT1;7* was preferentially expressed in source leaves and nodes. A further fine-localization analysis by immunostaining showed that *OsPHT1;7* expression was restricted in the vascular bundle (VB) sheath and phloem of source leaves as well as in the phloem of regular/diffuse- and enlarged-VBs of nodes. In accordance with this expression pattern, mutation of *OsPHT1;7* led to increased and decreased P distribution in source (old leaves) and sink organs (new leaves/panicles), respectively, indicating that OsPHT1;7 is involved in P redistribution. Furthermore, *OsPHT1;7* showed an overwhelmingly higher transcript abundance in anthers than other PHT1 members, and *ospht1;7* mutants were impaired in P accumulation in anthers but not in pistils or husks. Moreover, the germination of pollen grains was significantly inhibited upon *OsPHT1;7* mutation, leading to a >80% decrease in seed-setting rate and grain yield. Taken together, our results provide evidence that OsPHT1;7 is a crucial Pi transporter for Pi transport and recycling within rice plants, stimulating both vegetative and reproductive growth.

Introduction

Phosphorus (P) is an essential macronutrient indispensable for plant growth and development, serving as a constituent of many biologically important molecules such as phospholipids, nucleic acids, and P-containing proteins and

carbohydrates (Raghothama, 1999; Wang et al., 2021a). Mined rock phosphate (Pi) is the predominant source for P fertilizers. Unlike nitrogen, however, rock Pi is a nonrenewable resource and has been estimated to be exhausted within several decades to four hundred years (Oelkers and Valsami-Jones, 2008; Van Kauwenbergh, 2010). To cope with the lack and/or fluctuation of this nutrient, plants have evolved an array of adaptive strategies involving diverse metabolic and morphological changes (Lambers and Plaxton, 2015; Gu et al., 2021; Liu, 2021; Wang et al., 2021b). On the other hand, the excessive use of P fertilizers in agricultural production results in severe environmental pollutions. Thus, there is an urgent need to reduce the dependence on P fertilizers, a major solution to which is to improve crop P efficiency.

Crop P efficiency is classified into two categories, namely P acquisition efficiency (PAE) and P use efficiency (PUE), both of which can be measured by a suite of different parameters (Hammond et al., 2009; Chen and Liao, 2017). PAE reflects the plant capacity to take up Pi from soil, while PUE encompasses a wide range of physiological, structural, and developmental traits, all of which lay an effect on the distribution/redistribution of P among different organs/tissues (Veneklaas et al., 2012; Wang et al., 2019). To date, uneven attention has been paid to PAE over PUE, with much work focused on the mechanisms of root Pi uptake, which is closely related to PAE and heavily relies on the Pi Transporter 1 (PHT1) members (Ayadi et al., 2015); however, the mechanisms underlying the transport and recycling of P within plants, which is vital for improving crop PUE, remain poorly understood. Plant internal P recycling (P redistribution) is comprised of several steps, namely, breakdown or replacement of organic P, export of vacuolar P into cytoplasm, and transport of P from old organs to young and/or actively growing parts (Xu et al., 2019; Cong et al., 2020; Wang et al., 2020). The latter two steps require the coordination of Pi transporters (PTs) from different families.

Membrane transporters have been recognized as key factors for potentially improving crops and increasing sustainable food production (Schroeder et al., 2013; Gu et al., 2016). In angiosperms, most of the reported PHT1 genes are expressed in roots (Shin et al., 2004; Ai et al., 2009; Jia et al., 2011; Remy et al., 2012; Wang et al., 2014; Ye et al., 2015; Zhang et al., 2015, 2021; Chang et al., 2019), and it has been established that PHT1 proteins are probably the only influx transporter for Pi uptake (Ayadi et al., 2015). In addition, PTs belonging to the SYG1/PHO81/XPR1-Major Facilitator Superfamily (also known as the Vacuolar Pi Transporter or PHT5) family and the Glycerol-3-Pi Transporter family are responsible for the Pi transport into and out of vacuole across the tonoplast (vacuolar membrane) in response to sufficient Pi and deficient Pi, respectively (Wang et al., 2012, 2015, 2021c; Liu et al., 2015, 2016; Xu et al., 2019). As compared with the documented findings regarding the transporters for Pi uptake and subcellular Pi transport across tonoplast, the knowledge on the intercellular Pi transport during P redistribution is still limited, especially that at the cellular resolution. In Arabidopsis (Arabidopsis thaliana), AtPHT1;5 is expressed in the phloem of vascular bundles (VBs) of senescing leaves, and mediates P redistribution from source leaves to sink organs (Mudge et al., 2002; Nagarajan et al., 2011). In barley (Hordeum vulgare), HvPHT1;6 expression is mainly restricted to the phloem of VBs of old leaves, and has been suggested to play a role in P redistribution (Rae et al., 2003; Preuss et al., 2010). Recently, we functionally characterized a PHT1 member in rice (Oryza sativa), OsPHT1;3. OsPHT1;3 is specifically expressed in the phloem of both regular VB (RVB; P_R) and enlarged VB (EVB; P_E) of basal nodes, and it is responsible for P redistribution from old to young leaves (Chang et al., 2019). Despite this progress, several open questions remain regarding the mechanisms underlying P redistribution at the physiological and molecular levels: (1) Does the translocation of Pi from mesophyll cells (MCs; the major P storage cells in monocots) to bundle sheath (BS; a cell layer surrounding the VB serving as an apoplastic barrier) and then to the phloem parenchyma cells (PPCs)/companion cells (CCs) in source leaves (short-distance transport) undergo symplastic pathway or apoplastic pathway or both? (2) If symplastic pathway is involved, what is the driving force for the afore-mentioned short-distance transport? (3) To what extent does the "pressure-flow hypothesis" for sugar movement in phloem fit to P redistribution; (4) If apoplastic pathway is required, which transporters are responsible for Pi export from MCs and Pi influx into BS cells and PPCs/CCs?

The anther is a plant reproductive organ producing the male gamete, pollen, thus its development is an important determinant for crop yield maintenance. In rice, within ten days prior to flowering, a >10-fold increase in anther Pi content has been reported (Yamada, 1972). However, the biological role of this Pi accumulation in anther and the PTs mediating Pi influx into anther are still unclear. AtPHT1;6 is mainly transcribed in anthers and mature pollen grains; strong expression of AtPHT1;7 is also observed in mature pollen grains (Mudge et al., 2002). However, their roles in anther P accumulation and the potential physiological impact on reproductive growth are unknown.

Many PHT1 genes are broadly expressed throughout plants in addition to roots, making a specific role in a certain biological process unlikely (Wang et al., 2016). Indeed, several lines of evidence show that some PHT1 members participate in at least two biological processes involving intercellular Pi transport (Ai et al., 2009; Chang et al., 2019). In addition, several constraints in previous studies signify the necessity for further investigations: (1) the lack of fine-localization analysis of PTs at the cellular resolution and insufficient anatomic analysis might compromise the understanding of the Pi transport processes and (2) the information regarding the physiological roles of PTs at reproductive stage is lacking. In the present work, we functionally characterized a rice PHT1 gene, OsPHT1;7 (PHT1;7 hereafter), preferentially expressed in shoot organs. Our results

demonstrate that the apoplastic pathway is required for P redistribution during which PHT1;7 exerts its function in the BS and PPCs/CCs of source leaves and in nodes, and that PHT1;7-mediated anther P accumulation is vital for yield maintenance.

Results

PHT1;7 responds to Pi starvation in the shoot basal region and old leaf and shows the highest expression level in anthers

At the very beginning of this work, we failed to detect any expression of *PHT1;7* in the roots and the young leaves of rice seedlings subjected to either high P or low P treatments. This prompted us to speculate that: (1) *PHT1;7* is a pseudo-gene or (2) it is expressed in certain cell types and/or is in-duced by (an) unknown stimulus/stimuli. To test these speculations, we split the shoot into individual leaves and shoot basal region (SBR; composed of basal node and the basal part of leaf sheaths [LSs]). Reverse transcription-quantitative polymerase chain reaction (RT-qPCR) analysis showed that *PHT1;7* was barely expressed in root and the two new leaves (leaves 6 and 7), whereas strong expression was detected in SBR and old leaves (leaves 3–5). *PHT1;7* was transcriptionally induced by low P stress in all the tissues where it was expressed except in leaf 5 (Figure 1A).

At the reproductive stage, *PHT1;7* showed a moderate ex-pression level in leaf blade II (LBII) and flag LB (FLB), and a much higher abundance in spikelet (Figure 1B). To further investigate the expression pattern of *PHT1;7* in spikelet, we dissected the spikelet into husk, anther, and pistil, and found that *PHT1;7* was mainly transcribed in anther (Figure 1C), consistent with the microarray data obtained from the RiceXPro database (Supplemental Figure S1; http://ricexpro.dna.affrc.go.jp/; Sato et al., 2013). In addition, *PHT1;7* showed the highest transcript abundance in anther among the PHT1 family members (Figure 1D), suggesting its crucial role in this organ. We also examined the expression of *PHT1;7* at different seed developmental stages (just before anthesis [0 days], 3, 7, 14, 21, 28, 35, and 42 d after anthesis), and found that it was highly expressed at Day 0, whereas its ex-pression became almost undetectable from 3 d after anthesis onwards (Supplemental Figure S2). Given that anthers un-dergo dehiscence to release pollens, leading to anther struc-ture collapse, the results further demonstrated that PHT1;7 is mainly expressed in anthers.

PHT1;7 localizes in the plasma membrane and mediates Pi transport in yeast and *Xenopus* oocytes

To investigate the subcellular localization of *PHT1;7*, its full-length open reading frame was fused with the enhanced GFP (eGFP) reporter. Three constructs, *Pro35S:PHT1;7-eGFP*, *Pro35S:eGFP* and *Pro35S:OsRac1-mCherry*, were transfected into rice protoplasts alone or in pairs. The results showed that the eGFP alone was universally distributed inside the cell except for the vacuole, whereas the green fluorescence signal derived from the PHT1;7–eGFP fusion overlapped

with the red fluorescence transmitted by the OsRac1–mCherry fusion, which serves as a marker for plasma mem-brane (Figure 2A; Ono et al., 2001). This indicates that PHT1;7 is a plasma membrane-localized protein. Given that reported PHT1 proteins and other transporters often show localization to intracellular compartments (e.g. cytoplasm, nucleus, endoplasmic reticulum, or vesicles) in addition to plasma membrane (Bayle et al., 2011; Ueno et al., 2015), we further investigate the subcellular localization of PHT1;7 by monitoring different planes of a cell via z-stack scanning. Similar to the reported findings, the fluorescent signals emit-ted by PHT1;7-eGFP and OsRac1-mCherry were both detected in plasma membrane and intracellular compart-ments. The eGFP signal co-localized with the mCherry signal in plasma membrane, and the two fluorescent signals largely overlapped in the intracellular compartment(s) as well, al-though in some planes the intracellular signal was only evi-dent for eGFP but not mCherry (Supplemental Figure S3). Nevertheless, all these results suggest that PHT1;7 localizes to plasma membrane.

Two heterologous systems were utilized to examine the potential transport activity of PHT1;7 for Pi. A yeast mutant defective in five PTs (PHO84, PHO89, PHO87, PHO90, and PHO91), EY917 (Wykoff and O'Shea, 2001; Wang et al., 2015), was transformed with *PHT1;7* under the control of a constitutive promoter (*ProGPD*; glycerol-3-phosphate dehy-drogenase). In addition, another rice PHT1 member, *OsPHT1;8*, was used as a positive control, since it has been demonstrated to mediate Pi uptake in yeast under a wide range of external Pi levels (Chang et al., 2019). When galac-tose was supplied as the carbon source, the yeast PT gene *PHO84* which is driven by a galactose-inducible promoter was expressed, thus the yeast mutants transformed with the empty vector (EV), *ProGPD:OsPHT1;8*, or *ProGPD:PHT1;7* all grew normally (Figure 2B). When glucose was used as the carbon source, the yeast mutant transformed with EV did not show any growth under all Pi regimes, whereas those transformed with *ProGPD:OsPHT1;8* showed normal growth. The growth of the yeast mutant complemented with *PHT1;7* was restored irrespective of the external Pi levels, al-though the growth rate was slightly slower than that com-plemented with *OsPHT1;8* (Figure 2B). The transport activity of PHT1;7 for Pi was assessed also in *Xenopus laevis* oocytes with radioactive ^{32}P. The oocytes injected with *PHT1;7* cRNA showed significantly higher accumulation of ^{32}P com-pared with that injected with water at pH 5.5; however, at pH 7.4, no obvious transport activity was observed (Figure 2C). These results indicate that PHT1;7 is a Pi/H$^+$ symporter.

Tissue localization analysis of *PHT1;7*

To further analyze the expression pattern of *PHT1;7*, a geno-mic sequence upstream of its translation start site with a length of 2,315 bp was fused to the GUS reporter, generat-ing the *ProPHT1;7:GUS* transgenic rice plants. We first inves-tigated *PHT1;7* expression pattern at seedling stage. The same as that found in the RT-qPCR analysis, GUS activity
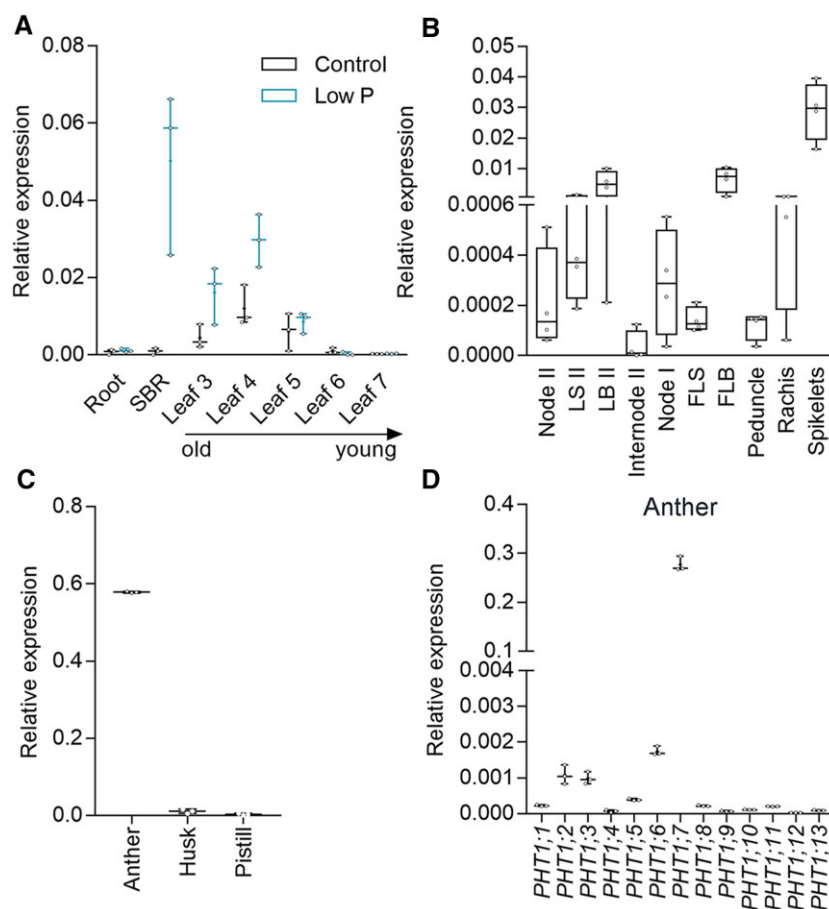
Figure 1 Temporal and spatial expression of *PHT1;7* and expression of *PHT1* family genes in rice anthers. A, Relative expression of *PHT1;7* in root, SBR and leaves (leaves 3–7) of seven-leaf-old seedlings treated with control (90 μM Pi) or low P (1 μM Pi) nutrient solution for 14 d since the fourth leaf appeared. B, Relative expression of *PHT1;7* in different tissues, including the node II, LS II, LB II, internode II, node I, flag LS, FLB, peduncle, rachis, and spikelet, that were sampled from rice cultivated in a paddy field 1 d before anthesis. C, Relative expression of *PHT1;7* in floral organs, including the anther, husk, and pistil, collected from spikelets 1 d before anthesis. D, Relative expression of rice *PHT1* family genes (13 members) in rice anthers. Gene expression level was determined by RT-qPCR. *OsActin1* (LOC_Os03g50885) was used as an internal control. All data are plotted with box and whiskers plots: whiskers plot represents minimum and maximum values, and box plot represents second quartile, median and third quartile.

was observed in leaf and basal node but not in root (Supplemental Figure S4; Figure 1A). To investigate the fine cellular localization of *PHT1;7*, an immunostaining analysis was performed. In LB, GUS activity was not detected in epidermal cells (including bulliform cells and stomatal cells), MCs or the sclerenchyma cells (SCs) neighboring the VBs (Figure 3A); in contrast, strong *PHT1;7* expression was observed in the vascular BS cells as well as in the PPCs and CCs (Figure 3, A and B). In basal node, *PHT1;7* expression was restricted in the P_R and P_E (Figure 3, C and D). Notably, the Pi availability does not change the spatial expression pattern of *PHT1;7*, except that its transcription was weaker under Pi-sufficient condition, consistent with the RT-qPCR results (Supplemental Figure S4; Figures 1 and 3). Subsequently, *PHT1;7* expression pattern was examined at reproductive stage as well. In node I, *PHT1;7* was expressed in the P_E and diffuse VB (DVB [P_D]; Figure 3, E–G). In addition, strong GUS activity was also detectable in anther and pollen grain (Figure 3, H and I).

PHT1;7 is involved in P redistribution from source to sink tissues

To investigate the physiological roles of *PHT1;7*, we first generated *pht1;7* mutant lines by the clustered regularly interspaced short palindromic repeats/CRISPR-associated 9 (CRISPR-Cas9) system by using three independent spacers (Supplemental Table S1; Supplemental Figure S5) and subjected the mutants and wild-type (WT) plants to high Pi (HP: 90 μM Pi) and low Pi (LP: 1 μM Pi) treatments. We then determined the Pi concentration in root, SBR, and each individual leaf. Higher Pi concentration was observed in the old leaves but not young leaves of *pht1;7* mutants under both HP (leaf 4/5) and LP (leaf 3/4) conditions compared with that of the WT plants (Figure 4). This result suggests that, upon *PHT1;7* mutation, more Pi was distributed to older leaves, and/or less Pi was redistributed from older leaves to sink tissues. Given the phloem localization of *PHT1;7* in the VBs of leaf and basal node (Figure 3), we favored the latter assumption and reasoned that PHT1;7 is
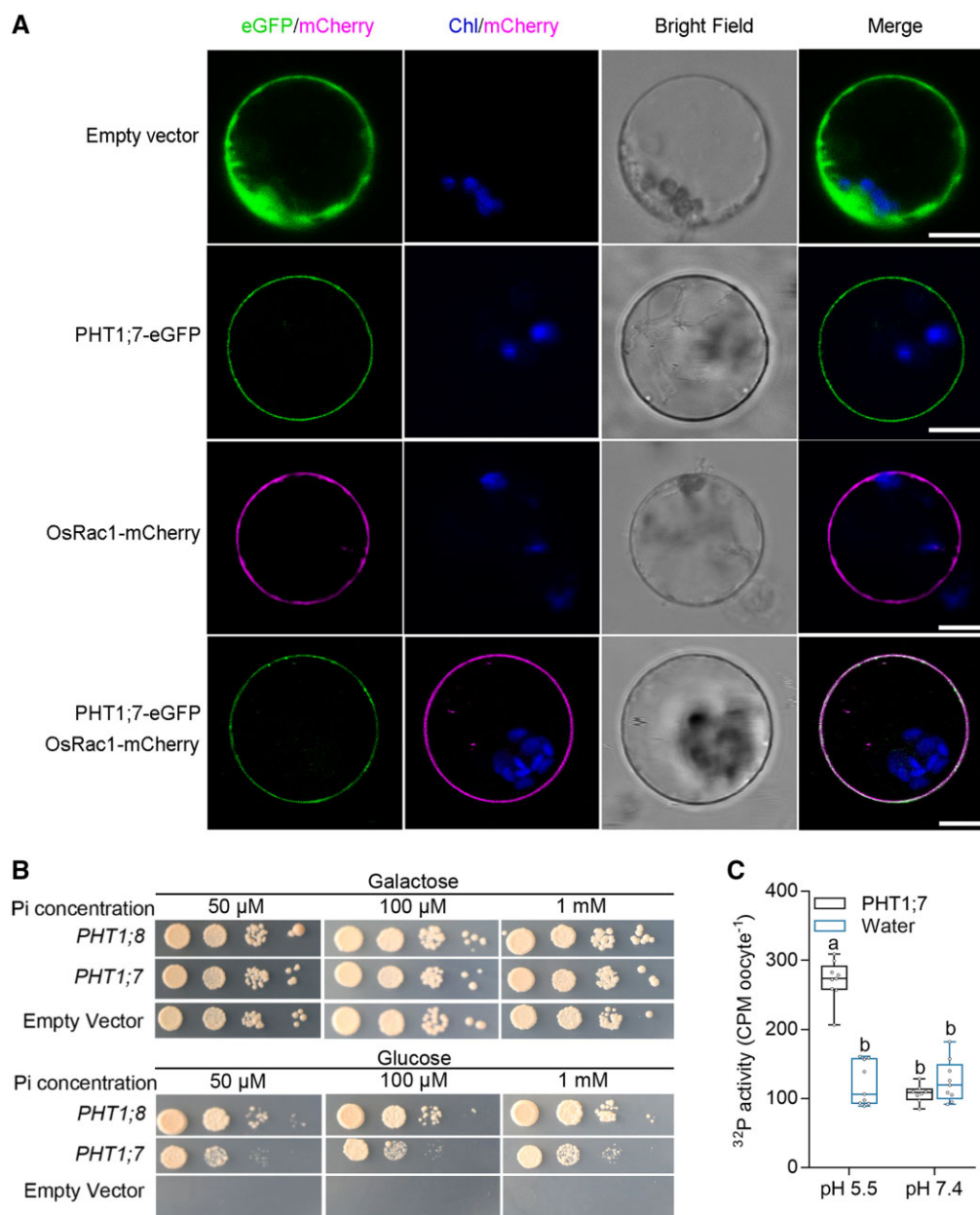
Figure 2 Subcellular localization of PHT1;7 and evaluation of the Pi transport activity of PHT1;7 in yeast and oocytes. A, Plasma membrane localization of PHT1;7 in the rice protoplast. PHT1;7 was colocalized with the plasma membrane-localized GTPase OsRac1. Scale bars = 10 μm. B, Complementation of a yeast mutant EY917 (Δpho84Δpho87Δpho89Δpho90Δpho91) defective in Pi uptake by PHT1;7. Yeast cells harboring either PHT1;8 construct (positive control) or PHT1;7 construct and an EV (negative control) were grown in synthetic dropout (-Trp/-Ura) liquid medium containing 2% (w/v) galactose to an optical density at the wavelength of 600 nm (OD$_{600}$) of 1. Then 5-μL aliquots of 10-fold serial gradient dilutions were spotted on agar plates with galactose or glucose as carbon source containing different Pi concentration, respectively. Plates were incubated at 28°C for 4 d. C, Transport activity of Pi in X. laevis oocytes. Oocytes expressing PHT1;7 or water-injected negative control were exposed to culture solution containing 0.5 mM Pi labeled with ^{32}P for 3 h at pH 5.5 or 7.4. Data in C are plotted with box and whiskers plots: whiskers plot represents minimum and maximum values, and box plot represents second quartile, median, and third. Different letters indicate significant differences ($P < 0.05$, one-way analysis of variance, Duncan's test).

involved in P redistribution. A similar phenomenon has been reported also in an Arabidopsis mutant defective in nitrate remobilization, nrt1.7, which accumulates more nitrate in old leaves but an equal level of nitrate in young leaves (Fan et al., 2009). Collectively, we speculated that, the impaired nutrient (i.e. Pi or nitrate) remobilization in old leaves and/or the enhanced nutrient demand in young leaves may trigger a downward systemic signal, leading to elevated nutrient uptake. To test this speculation, we examined the expression of other PHT1 genes in pht1;7 mutants.
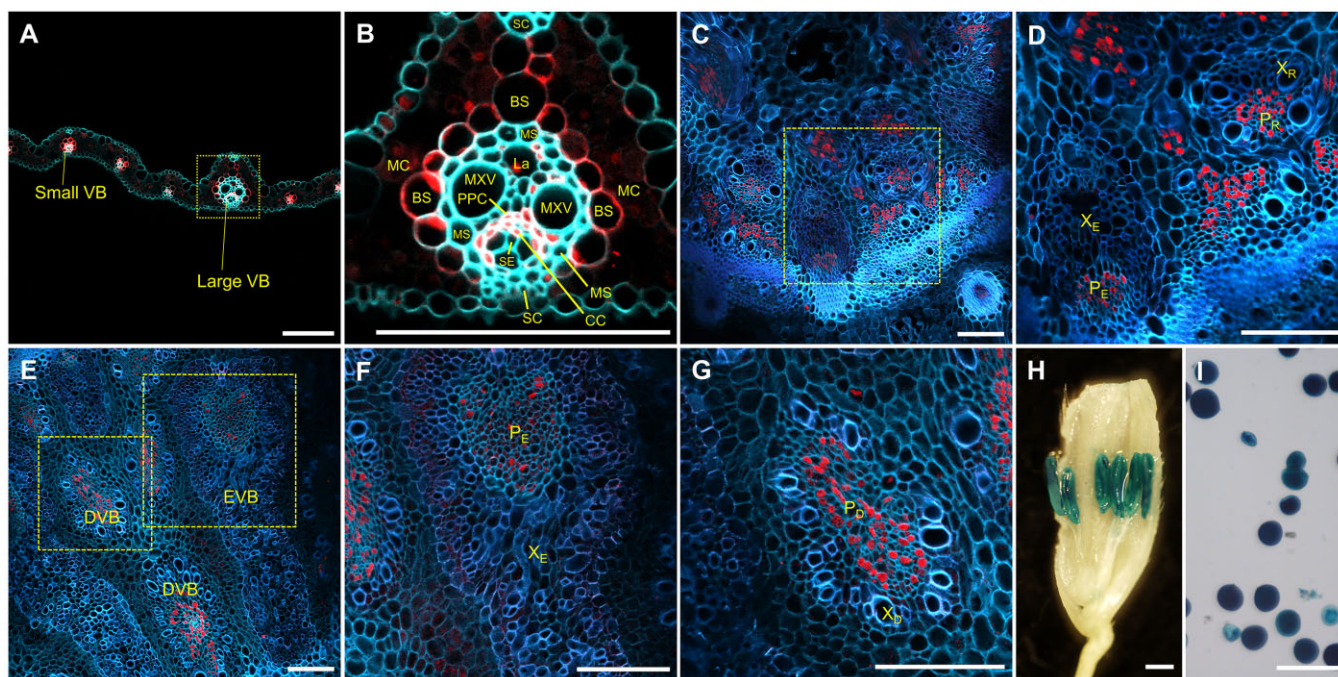
Figure 3 Tissue-specific localization of PHT1;7 as indicated by the GUS reporter gene of transgenic rice plants harboring *ProPHT1;7:GUS* fusion construct. A–G, Immunostaining of the cross sections of old leaf blade (A and B), basal nodes (C and D), and node I (E–G) using an anti-GUS antibody, respectively. The cyan or blue color in (A–G) represents autofluorescence of cell walls, the red color in (A–G) represents location of *ProPHT1;7:GUS*. H and I, Histochemical staining for GUS activity in anthers and pollen grains of transgenic plants, respectively. Samples in (A–D) were collected from plants grown in nutrient solution containing 1-μM Pi for 14 d since the fourth leaf appeared, and samples in (E–I) were collected from plants grown in the paddy field. MXV, metaxylem vessel; La, protoxylem lacuna; X_R, xylem of RVB; X_D, xylem of DVB. Scale bars = 100 μm in (A)–(G), (I) and 1 mm in (H).

Unexpectedly, no consistent alteration in the expression of these PHT1 genes was found in *pht1;7* mutants (Supplemental Figure S6). Thus, this enhancement in P accumulation might be achieved through a yet to be identified mechanism but not the transcriptional upregulation of PHT1 genes.

To validate the potential role of PHT1;7 in P redistribution, *pht1;7* and WT seedlings were first grown in Pi-sufficient solution until the emergence of the sixth leaf from the LSs of older leaves, and then subjected to nutrient solution lacking Pi. The roots, SBRs, and individual leaves of each genotype were collected prior to the Pi-starvation treatment and at the developmental stages when the seventh and eighth leaves emerge. Upon the Pi starvation treatment, more P was distributed to the SBR and old leaves (leaves 4 and 5) of *pht1;7* mutant lines compared with that in WT plants at both time points (Figure 5). In addition, a 1-week treatment led to a marginal decrease in P distribution to the youngest leaves (leaf 7) of *pht1;7* mutants, whereas after another 1-week treatment, a significant decrease in P distribution to the youngest leaves (leaf 8) of *pht1;7* was detected (Figure 5). Altogether, these results demonstrate that PHT1;7 is involved in P redistribution from source (old leaf) to sink (the youngest leaf) tissues at seedling stage in response to Pi starvation stress.

PHT1;7 is involved in P redistribution from vegetative organs to reproductive organs

At the ripening stage, the plant height and panicle length of *pht1;7* mutants were reduced to ~82.9% and ~83.2% of that of WT plants, respectively (Figure 6, A–D). Since *PHT1;7* is expressed in the P_D and P_E of node I (Figure 3, E–G), the stunted growth may result from impaired P redistribution. To test this hypothesis, we determined the P concentration in different organs of *pht1;7* mutants and WT plants at mature-grain stage. A higher P concentration was observed in almost all the organs (including brown rice, the sink) of *pht1;7* mutants compared with that of WT plants (Supplemental Figure S7A). This is probably attributed to the dramatic decrease ($>$80%) in seed-setting rate and grain yield (Figure 6, E and F), which attenuated the sink strength and led to enhanced distribution of P taken up to vegetative organs (i.e. an indirect effect of less P flow to grains). Nevertheless, the P distribution to panicles was significantly decreased in *pht1;7* mutants (Supplemental Figure S7B). To avoid the large differences in sink strength between *pht1;7* mutant lines and WT plants, we analyzed the P accumulation in different organs at the onset of flowering stage. The P concentration in the leaf II and flag leaf of *pht1;7* mutants was significantly higher than that of WT plants (Supplemental Figure S8A). In addition, upon *PHT1;7*
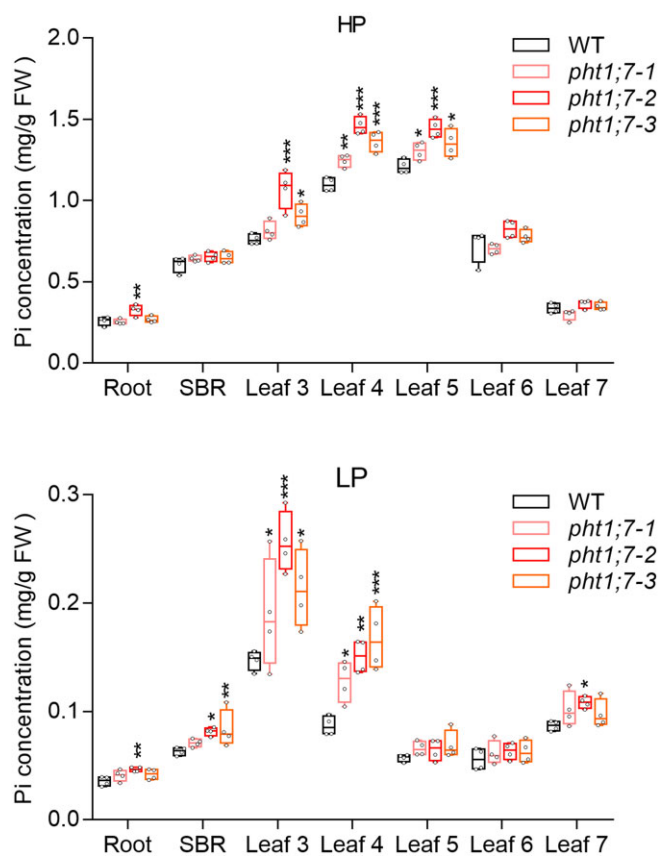
Figure 4 Pi concentrations of tissues of WT and *pht1;7* mutants in seedling stage after HP (90 μM Pi) or LP (1 μM Pi) treatments. Four-leaf-old seedlings were grown in 1/2 Kimura nutrient solution supplied with HP or LP until the seventh leaf appeared. Each treatment contains four biological replicates and each replicate contains tissues of two seedlings. All data are plotted with box and whiskers plots: whiskers plot represents minimum and maximum values, and box plot represents second quartile, median, and third quartile. Asterisks indicate significant differences (*$P < 0.05$; **$P < 0.01$; ***$P < 0.001$) compared with the WT, one-way analysis of variance, Duncan's test.

mutation, the P distribution was increased and decreased, respectively, in leaf II and panicle (Supplemental Figure S8B). These results together with the phloem localization of *PHT1;7* in nodes (Figure 3, E–G) suggest that PHT1;7 is involved in P redistribution from source (leaf) to sink organs (panicle) at reproductive stage as well.

Mutation of *PHT1;7* leads to an impairment in anther P accumulation, pollen grain germination, and fertility

Given that *PHT1;7* was highly expressed in anther (Figure 1, C and D) and that *pht1;7* was impaired in fertility (Figure 6E), we speculated that PHT1;7 might maintain the fertility through regulating the P accumulation and development of anther. The results showed that the length and P concentration of anther were both significantly decreased due to *PHT1;7* mutation (Figure 7). In addition, the pollen viability of *pht1;7* mutants was disturbed, as evidenced by a sharp decrease in starch granules (SGs) in pollen grains

(Figure 8A). Consistently, the proportion of fully stained pollen grains by KI–I$_2$ was markedly reduced in the *pht1;7* mutant lines as compared with that in WT plants (Figure 8, B and C). As a consequence, the in vitro and in vivo germination of pollen grains were all impaired in *pht1;7* mutants (Figure 9).

Discussion

OsPHT1;7 is a major PT responsible for Pi transport into anther and pollen viability maintenance

The germination of pollen grains involves drastic cell proliferation/expansion and thus consumes plenty of energy and nutrients including Pi. In rice, Pi concentration in anthers undergoes a 10-fold increase within 10 d prior to flowering (Yamada, 1972), during which *PHT1;7* transcript level is concurrently elevated in anther (Lin et al., 2017). Given that PHT1;7 is a plasma membrane-localized PT (Figure 2), it is very likely that PHT1;7 is involved in the storage of Pi in anthers/pollens. In support of this presumption, mutation of *PHT1;7* led to a significant decrease in anther P accumulation (Figure 7C). Interestingly, *PHT1;7* showed an overwhelmingly higher transcript level than other PHT1 counterparts (Figure 1D), yet the decrease in anther P accumulation in *pht1;7* mutants was not that severe as expected (∼20%; Figure 7C). This indicates a gene functional redundancy and/or potential genetic complementation of *PHT1;7* by other PT genes. Indeed, several PHT1 genes showed relatively low but non-negligible expression in anthers (Figure 1D). In addition, two PHT1 members, namely *OsPHT1;1* and *OsPHT1;6*, were upregulated in the anthers of *pht1;7* mutants compared with that of the WT plants (Supplemental Figure S9). Notably, the expression level of *OsPHT1;1* in *pht1;7* anthers was two to 3 times as high as that in WT anthers; in contrast, the transcript abundance of *OsPHT1;6* in anthers was increased >30-folds upon *PHT1;7* mutation (Supplemental Figure S9). This suggests a more important complementary role of OsPHT1;6 in mediating Pi influx into anthers than OsPHT1;1 when PHT1;7 function is lost. In future work, the potential role of OsPHT1;6 in anther P accumulation and anther development needs to be investigated.

The decrease in the anther P accumulation in *pht1;7* mutants was accompanied by a dramatic impairment in pollen grain viability (Figures 7–9). A conventional parameter reflecting pollen viability is the content of starch, the biosynthesis of which is catalyzed by several enzymes, including plastidic phosphoglucomutase (pPGM; transform glucose-6-Pi into glucose-1-Pi) and ADP-glucose pyrophosphorylase (AGP; transforming glucose-1-Pi into ADP-glucose, the precursor of starch). *OspPGM* and *OsAGPL4* encode the major pPGM and AGP, respectively, functioning in rice pollens (Supplemental Figure S10A; Lee et al., 2016; Meng et al., 2020). In the anthers of *pht1;7* mutants, *OsAGPL4* expression was unaltered, whereas *OspPGM* was significantly upregulated compared with that of the WT plants (Supplemental Figure S10B). Given that the starch content was reduced in *pht1;7* anthers, this increase in *OspPGM* expression upon
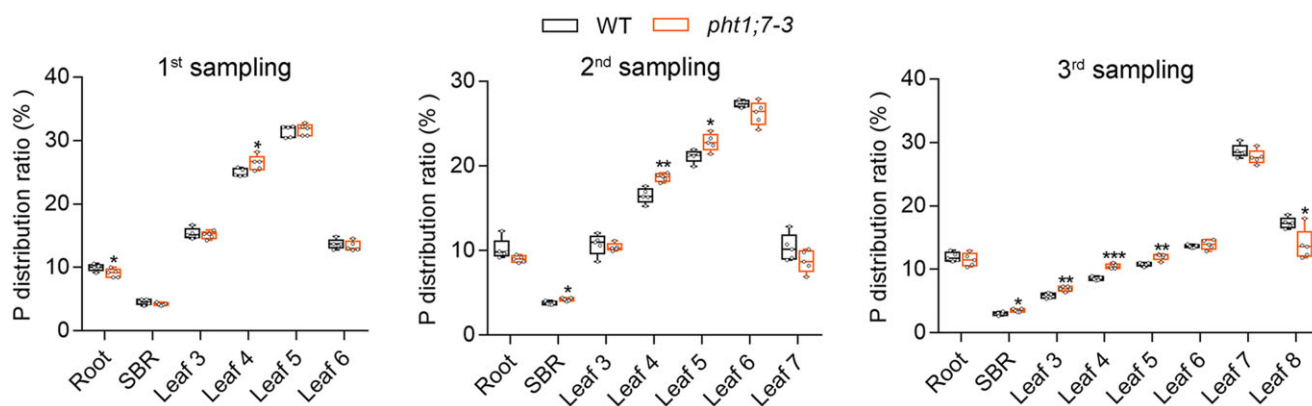
Figure 5 *PHT1;7* is involved in P redistribution from source to sink tissues in seedling stage. The WT and the *pht1;7* mutant plants were treated with nutrient solution of 90-μM Pi till leaf 6 appeared, and tissues were collected for the first time (first sampling). Whereafter, the WT and the *pht1;7* mutant plants with uniform growth condition were transferred to nutrient solution of no Pi. Tissues of the WT and the *pht1;7* mutant plants were collected for the second time (second sampling) when the leaf 7 of the WT appeared. After continuing for several days of no Pi treatment, tissues of the WT and the *pht1;7* mutant plants were collected for the third time (third sampling) when the leaf 8 of the WT appeared. Leaf 3 indicates the oldest leaf, and leaf 8 indicates the youngest leaf. P distribution ratio in different tissues of the WT and *pht1;7-3* mutant was calculated by P content in each tissue divided by P content in the whole plant. Each treatment contains five biological replicates and each replicate contains tissues of two seedlings. All data are plotted with box and whiskers plots: whiskers plot represents minimum and maximum values, and box plot represents second quartile, median and third quartile. Asterisks indicate significant differences (*$P < 0.05$; **$P < 0.01$; ***$P < 0.001$) compared with the WT, one-way analysis of variance, Duncan's test.
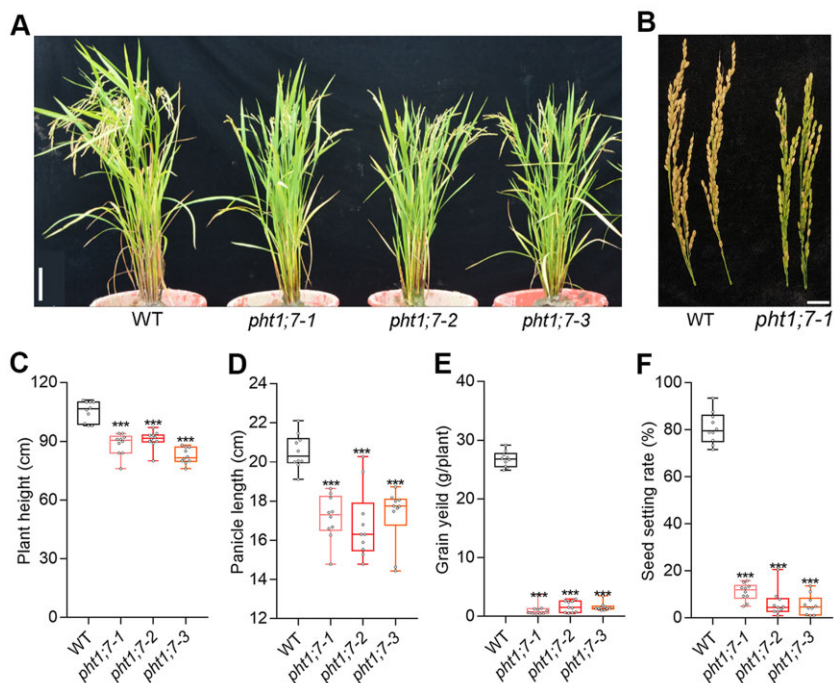

Figure 6 Plant performance and agronomy index of WT and *pht1;7* mutants at ripening stage. A and B, Phenotypes of whole plants and panicles. Scale bars = 10 cm in (A) and 2 cm in (B). C–F, Plant height, panicle length, seed setting rates, and grain yield per plant of WT and *pht1;7* mutants, $n = 10$. All data in (C–F) are plotted with box and whiskers plots: whiskers plot represents minimum and maximum values, and box plot represents second quartile, median and third quartile. Asterisks indicate significant differences (***$P < 0.001$) compared with the WT, one-way analysis of variance, Duncan's test.

PHT1;7 mutation is probably an indirect effect. It would be of interest to know whether Pi serves as a signaling molecule or a nutritional basis or both to sustain the development of anthers/pollens.

Recently, it has been shown that a 40%–50% increase in anther Pi level in *osnla1* (*Nitrogen Limitation Adaptation 1*) mutants also resulted in lowered pollen viability (Yang et al. 2020). *OsNLA1* encodes a ubiquitin E3 ligase which
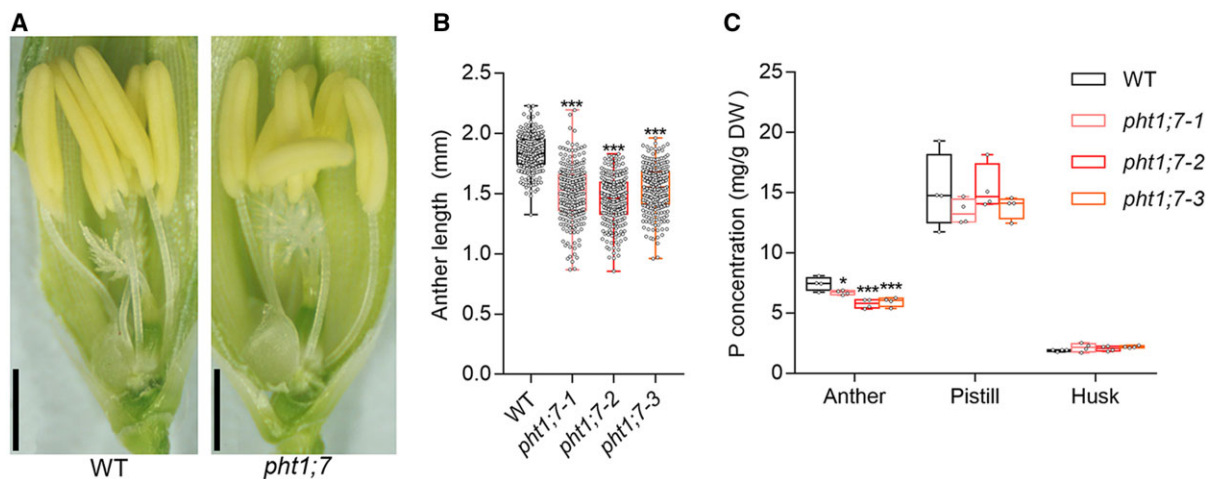
Figure 7 *PHT1;7* affects length and P concentration of anthers. A, Anther phenotypes of WT and a typical *pht1;7* mutant. Scale bars = 1 cm. B, Anther length of WT and *pht1;7* mutants, n = 200. C, Total P concentrations of anthers, pistil, and husk of WT and *pht1;7* mutants. Each tissue in (C) contains four replicates, and each replicate contains organs from ∼40 spikelets from tillers of five individual plants. Spikelet or anther samples in (A–C) were collected 1 d before anthesis from plants grown in a paddy field. All data in (B) and (C) are plotted with box and whiskers plots: whiskers plot represents minimum and maximum values, and box plot represents second quartile, median and third quartile. Asterisks indicate significant differences (*P < 0.05; ***P < 0.001) compared with the WT in each group, one-way analysis of variance, Duncan's test.
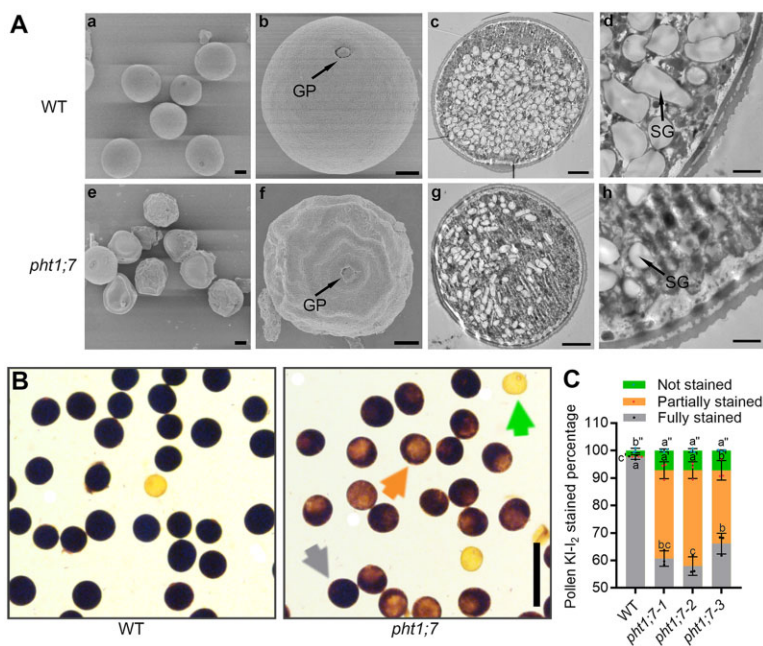

Figure 8 Morphological characteristics and viability assay of pollen grains in the WT and *pht1;7* mutants. A, Scanning and transmission electron micrographs of mature pollen grains from WT and *pht1;7* mutants. A(a)–(d) Micrographs of the WT pollen grains. A(e)–(h) Micrographs of *pht1;7* mutant pollen grains. Most of the pollen grains shown in (e) have an abnormal structure while pollen grains shown in A(a) have a rounded structure. Arrows in A(b) and A(f) point at germination pores of pollen grains. The WT pollen grains in A(c) and A(d) contain more SGs than the *pht1;7* pollen grain in A(g) and A(h). Scale bars = 10 μm in A(a) and A(e); 5 μm in A(b), A(c), A(f), and A(g); and 1 μm in A(d) and A(h). B and C, Pollen viability and percentage of each pollen category stained by KI–I₂ solution in WT and *pht1;7* mutant lines. Pollen grains were collected from flowering rice. The green, orange, and gray arrows point at not stained, partially stained, and fully stained pollen grains, respectively. Scale bars = 100 μm in (B). Data in (C) are means ± SD of three biological replicates. Different letters indicate significant differences (P < 0.05, one-way analysis of variance, Duncan's test).

maintains rice P homeostasis via negative regulation of the abundance of PHT1 proteins (Yue et al., 2017; Yang et al., 2020). Interestingly, *OsNLA1* is highly expressed in anthers as

well, and PHT1;7 has been demonstrated to be a direct target of OsNLA1 (Yang et al. 2020), suggesting that the increased Pi level in the anthers of *osnla1* is largely, if not
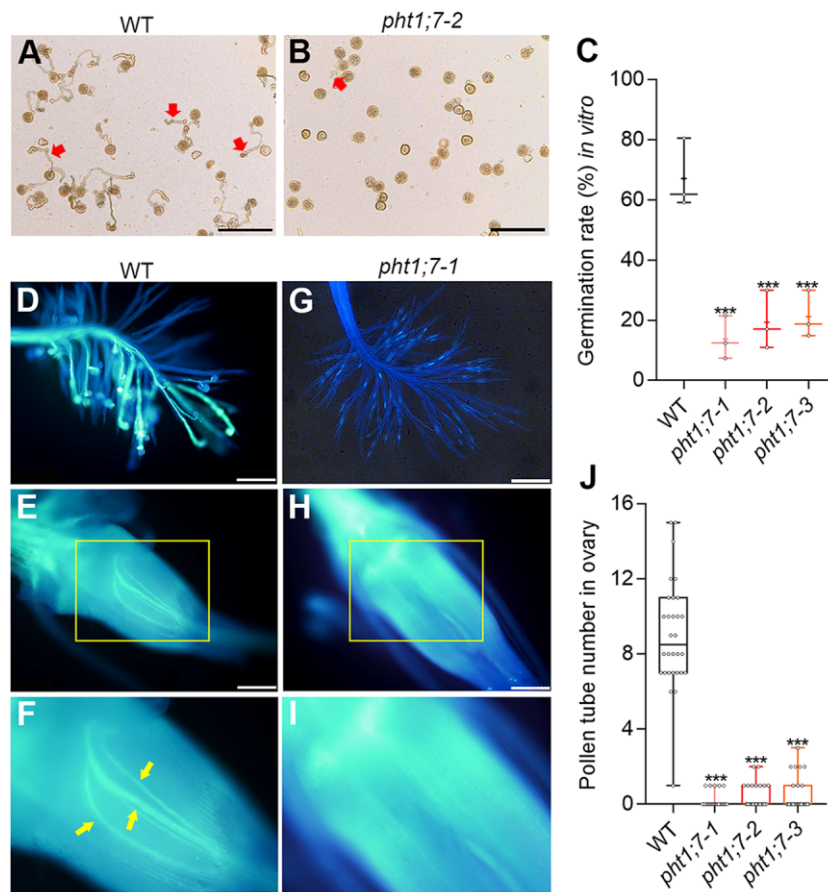
Figure 9 Pollen germination in vitro and in vivo. A–C, Pollen germination of WT and *pht1;7* mutants and germination rate in vitro. Mature pollen grains were collected at the onset of flowering and observed by a microscope after germinated 2 h in the pollen germination medium, *n* = 3. Each independent plant was used as one biological replicate, and pollen grains from more than five spikelets of each independent plant were checked. D–I, Pollen germination of WT and a typical *pht1;7* mutant line in vivo. (D) and (G) are stigmas of WT and the *pht1;7* mutant, respectively; (E) and (H) are ovaries of WT and *pht1;7* mutant, respectively; (F) and (I) are the enlarged exhibition of the area in yellow rectangles of (E) and (H), respectively. Yellow arrows in (F) point at pollen tubes in ovary. J, Pollen tube number in ovaries of WT and *pht1;7* mutants, *n* = 30. Spikelets for in vivo analysis were collected and mixed from five independent plant 2 h after flowering and then stained with aniline blue. All data in (C) and (J) are plotted with box and whiskers plots: whiskers plot represents minimum and maximum values, and box plot represents second quartile, median and third quartile. Asterisks indicate significant differences (***P < 0.001) compared with the WT, one-way analysis of variance, Duncan's test. Scale bars = 200 μm.

entirely, contributed by PHT1;7. Our results and the reported findings indicate that anther P level needs to be maintained in a narrow range to ensure normal development and functioning of anthers/pollens, and that PHT1;7 is indispensable for maintaining the P homeostasis in anther and the fertility of rice plants. Nevertheless, the possibility that PHT1;7 facilitates the transport of other unknown substrate(s) essential for pollen grain viability and anther development cannot be excluded.

P redistribution in source leaves involves the apoplastic pathway and requires the activity of PHT1;7 at two steps

The redistribution of P from source (e.g. mature leaf) to sink (e.g. young leaf) organs involves several sequential steps regarding intercellular Pi transport, namely (1) short-distance transport of Pi from outer cell layers (i.e. MCs) to BS cells;

(2) loading of Pi into the sieve element (SE)–CC complex; (3) downward long-distance transport of Pi from mature leaves to basal nodes through sieve tubes; and (4) upward distribution of Pi to sink leaves. *PHT1;7* is involved in P remobilization in response to Pi starvation stress (Figure 5), and it is specifically expressed in the BS cell layer and the PPC/CC of leaf VBs as well as in the P_R and P_E of basal nodes (Figure 3, A–D), indicating that PHT1;7 promotes P remobilization at multiple steps. BS is a ring of parenchymatous cells enclosing the VB, and is thus the interface between MCs and vasculature. It has been recognized as a "flux-regulating" tissue for retrieving, storing, and redirecting solutes via preventing apoplastic water/solute flow (Shatil-Cohen and Moshelion, 2012; Wigoda et al., 2014). Water and minerals from the transpiration stream need to cross BS to reach the MCs; likewise, water, ions, and other solutes (e.g. assimilates) flow through BS before phloem loading in

source leaves and after phloem unloading in sink organs. In the leaves of monocots, P is preferentially allocated to photosynthetic cells (i.e. MCs; Conn and Gilliham, 2010), indicating that MCs are an important P source for P redistribution and the P in MCs needs to be exported. The presence of plasmodesmata between the MCs and BS cells indicates that the symplastic pathway is implicated in the transport between these two cell types (Sage and Sage, 2009). However, the localization of PHT1;7 in the BS cell layer (Figure 3B) demonstrates that the apoplastic pathway is also required for the initial step of P remobilization (Step 1 as discussed above). Thus, the transporter responsible for Pi efflux from MCs into apoplast needs to be identified. Additionally, the potential contribution of the symplastic pathway (mediated by plasmodesmata between MCs and BS cells) to P remobilization at this step awaits to be investigated. In rice, mestome sheath (MS) is another single cell layer with thickened cell wall which is adjacent to the interior side of BS (Figure 3B), and there is no airspace at the BS–MS cell interface, and a symplastic transport at this interface has been inferred (Chonan et al., 1981; Leegood, 2008). PHT1;7 was not expressed in MS cells (Figure 3B). Thus, it is likely that the remobilized Pi undergoes symplastic pathway when flowing across the BS–MS interface. Furthermore, in many plants (e.g. Arabidopsis and herbaceous plants like rice), the phloem loading of sugar and amino acids into the SE–CC complex depend strongly on the apoplastic pathway (Regmi et al., 2016; Zhang and Turgeon, 2018; Wang et al., 2021d). This scenario is supported by the presence of H^+-pyrophosphatase, sucrose synthase, influx (AtSUC2) and efflux (AtSWEET11/12) sugar transporters, and amino acid transporter (AtAAP8) in the SE–CC complex (Stadler and Sauer, 1996; Chen et al., 2012; Regmi et al., 2016; Santiago and Tegeder, 2016). PHT1;7 expression was detected in the PPCs and CCs of the leaf vasculature as well (Figure 3B), indicating that another apoplastic transport event occurs at this step. Taken together, our results provide evidence that the apoplastic pathway is required for the phloem loading of Pi into SE, and that PHT1;7 functions at two steps in source leaves (BS and PPC/CC) for P remobilization. It remains to be established that whether the apoplastic Pi loading into the PPCs/CCs (and then into the SE) originates from the MCs or the cells within the vasculature or both.

PHT1;7 is not the only checkpoint for P redistribution in the phloem of the vascular bundles of nodes

The node is a highly specialized structure of graminaceous plants, functioning as a hub for the distribution of nutrients (Yamaji and Ma, 2014, 2017). At seedling stage, the internodes of rice plants are not elongated and all the nodes are compacted in the basal region of shoot, designated as basal nodes. In our previous work, we reported that a paralog of PHT1;7, OsPHT1;3, is specifically expressed in the P_D and P_R in response to Pi starvation. This expression pattern of OsPHT1;3 in basal nodes is almost the same as that of PHT1;7 (Figure 3, C and D) with the exception that OsPHT1;3 expression in the P_E is much weaker (Chang et al., 2019). Nevertheless, OsPHT1;3 and PHT1;7 are both involved in P redistribution from source to sink leaves in Pi-starved rice seedlings. OsPHT1;3 and OsPHT1;7 exert a similar role in P redistribution but not in anther development (Figures 4 and 5; Chang et al., 2019). This supports one of our previous presumptions that the physiological roles of transporters are largely determined by their spatio-temporal expression patterns rather than merely the similarities in their sequences and biochemical activities (Gu et al., 2016; further discussed in the section under the last subtitle), although the possibility that PHT1;7 is regulated by a distinct mechanism at posttranscriptional and/or posttranslational levels cannot be excluded.

At the reproductive stage of cereal plants, 60%–85% total plant P is finally allocated to the grains. In rice, the P in grains is derived from two pathways, namely the P newly taken up from soil after flowering stage and remobilization of P from old leaves. Yamaji et al. (2017) provide the first evidence that a rice plasma membrane PT, SULTR-like phosphorus distribution transporter (SPDT), which localizes to the xylem of and the parenchyma cell bridge between the DVB and EVB of node I, mediates the transient incorporation of Pi from xylem to the nodal tissues and promotes the xylem-to-phloem transfer of Pi in nodes. In addition, OsPHO1;2 is mainly expressed in the xylem of EVB (X_E) of node I, and mutation of this gene greatly inhibits the P accumulation/distribution and starch biosynthesis in rice grains (Che et al., 2020; Ma et al., 2021). Despite these striking findings, the PT(s) responsible for the phloem loading in nodes is/are widely unknown. A homolog of OsPHO1;2 sharing an amino acid sequence identity of 38.43%, OsPHO1;1, is mainly expressed in the P_D; however, its contribution to P accumulation in grains is limited, although the P distribution to grains is reduced upon its mutation (Che et al., 2020). This suggests that other phloem-localized PTs are involved in the P redistribution in nodes. OsPHT1;3 (Supplemental Figure S11, A–C) and PHT1;7 (Figure 3, E–G) are both expressed in the P_D and P_E of node I, indicating that they might serve as such PTs for phloem loading and mediate the remobilization of P to grains, functioning coordinately with SPDT and PHO1s in P accumulation in rice grains. However, mutation of OsPHT1;3 does not affect the P accumulation in brown rice (Supplemental Figure S11D), indicating a functional redundancy between OsPHT1;3 and other PT(s); the evaluation of PHT1;7 contribution to P accumulation in brown rice is impeded due to the greatly reduced seed-setting rate of pht1;7 mutants (Figure 6, B and F; Supplemental Figure S7). To fully dissect the rice grain P accumulation pathway in future work, it would be important to identify and functionally characterize the PT(s) playing a redundant role with OsPHT1;3 and PHT1;7 in the remobilization of P to grains. Particularly, given that the expression of OsPHT1;3 (Supplemental Figure S11, A–C) and PHT1;7

(Figure 3, E–G) in the P_E is weaker than that in the P_D of node I, the potential PT(s) showing a stronger expression in the P_E of node I could be an interesting target.

The functional conservation of *PHT1* genes is largely determined by their spatio-temporal expression patterns rather than amino acid sequence identities

The amino acid sequence identity between different members of a given protein-coding gene family within and among plant species is a major consideration when inferring their functional similarities. A high amino acid sequence identity between two homologs may indicate similar structure and biochemical activity. However, in many cases, it poorly reflects the conservation of physiological roles in plants, one major cause of which is the diverged spatio-temporal expression patterns of different homologs (Gu et al., 2016). *OsPHT1;1* is most closely related to *OsPHT1;2* and *OsPHT1;3* as shown by a phylogenetic analysis based on their amino acid sequences (Supplemental Figure S12). However, *OsPHT1;1* is constitutively expressed (not responsive to Pi starvation) and mainly involved in Pi uptake under Pi-replete conditions (Sun et al., 2012; Zhang et al., 2021), whereas *OsPHT1;2* and *OsPHT1;3* are both strongly induced by Pi starvation and responsible for Pi accumulation when Pi is lacking (Ai et al., 2009; Chang et al., 2019; Zhang et al., 2021). In addition, *OsPHT1;1* is not so phylogenetically related to *PHT1;7* (Supplemental Figure S12), yet *OsPHT1;1* showed a complementary upregulation in both node I and anther of *pht1;7* mutants (Supplemental Figures S9 and S13). Moreover, PHT1;7 shares the highest sequence identity with OsPHT1;6 (75.79%), and OsPHT1;6 might play a complementary role to PHT1;7 in Pi influx into anther (Supplemental Figure S9). Nonetheless, at vegetative stage, *OsPHT1;6* is expressed throughout rice plants and plays a broad role in Pi uptake and in planta transport (Ai et al., 2009); in contrast, *PHT1;7* showed preferential expression in the vascular tissues of leaves and basal nodes. Furthermore, the amino acid sequence identity between *PHT1;7* and *OsPHT1;3* is relatively low (70.57%), yet *OsPHT1;3* shows a highly similar expression pattern with *PHT1;7* in nodes, and these two genes both mediate P redistribution from source leaves to young leaves. Nevertheless, *OsPHT1;3* shows the highest expression level in roots and contributes to Pi uptake as well, whereas *PHT1;7* was barely expressed in roots (Figure 1A; Supplemental Figure S4, D and H; Chang et al., 2019). All these findings suggest that the spatio-temporal expression pattern of PHT1s is a major determinant of their physiological roles and functional redundancies. Given the importance of PTs for molecular breeding of crops with high P efficiency (Gu et al., 2016), in future work, the fine localization of PTs at the cellular resolution and at different developmental stages is of the utmost importance for the full understanding of their physiological roles, the prerequisite of practical application.
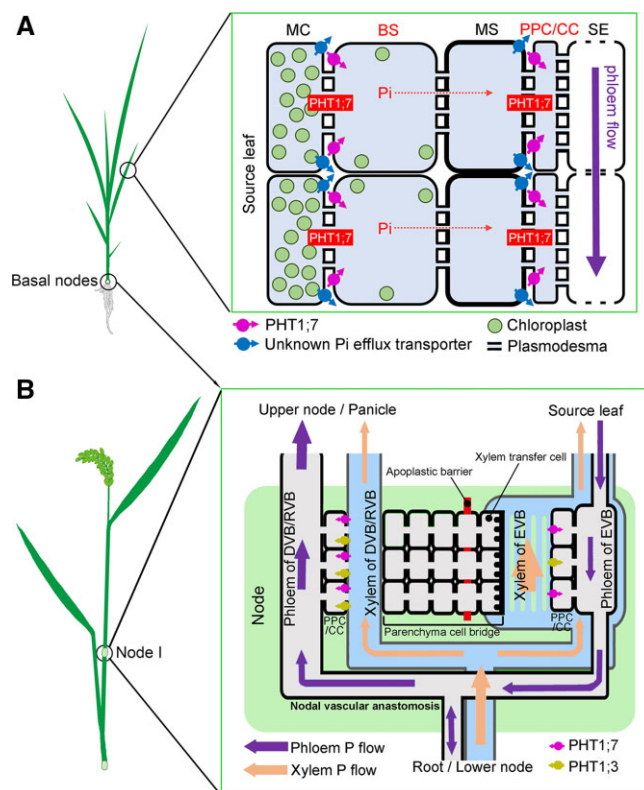
Figure 10 A working model for the roles of PHT1;7 in P redistribution in rice (O. sativa). A, Role of PHT1;7 in the short distance transfer of P in source leaf. P from mesophyll cells or MS cells is exported into apoplastic space by (an) unknown Pi efflux transporter(s). PHT1;7 located in VB sheath cells and CCs imports P from apoplast. P in CCs is further transferred to SEs through plasmodesmata. B, Role of PHT1;7 in nodes. P is loaded into the phloem in both EVBs and DVB/RVB by PHT1;7 and OsPHT1;3.

Conclusion

Our results show that PHT1;7 acts as a three-stage valve for P redistribution in (1) the BS and (2) PPC/CC of source leaves and in (3) the phloem of VBs of nodes (Figure 10), in response to Pi starvation stress, indicating that apoplastic transport is involved in P redistribution. Furthermore, we also demonstrate that PHT1;7 is required for anther development, pollen germination and yield formation.

Materials and methods

Plant materials and growth conditions

The rice (O. sativa) cultivar Nipponbare was used for experimental analysis and transgenic modification. For hydroponic experiments, seedlings were grown in a phytotron with a day/night photoperiod of 14/10 h and a day/night temperature of 30°C/24°C, and the relative humidity was controlled at 60%. Rice seeds were disinfected with 30% sodium hypochlorite (v/v, relative to the original solution) for 30 min, washed several times, and then incubated in sterile water in a 30°C dark environment to promote germination. After 48 h, seeds were placed on a nylon net floated on 0.5-mM $CaCl_2$ solution. When the first leaf was fully expanded,

seedlings were supplied with normal 1/2 Kimura B nutrient solution (Yamaji et al., 2013) till the fourth leaf appeared, and then treated with 1/2 Kimura nutrient solution of different Pi concentrations. For field experiments, all plants were grown in paddy fields with regular fertilization (400 kg urea, 35-kg P_2O_5, 130-kg K_2O/hectare) during the normal growing seasons in Nanjing, China.

RNA extraction, cDNA synthesis, and RT-qPCR

Samples were collected from plants in hydroponic condition or paddy fields, quick-frozen by liquid nitrogen and stored in a −80°C refrigerator till RNA extraction. Total RNA of plant samples except seeds was extracted using TRIzol reagent (Invitrogen, Thermo Fisher Scientific, Waltham, MA, USA) according to the manufacturer's instructions. Total RNA of seeds was extracted using RNAprep Pure Plant Plus Kit (Polysaccharides & Polyphenolics-rich, TIANGEN, Beijing, China) according to the manufacturer's instructions. First-strand cDNAs were synthesized from total RNA using the ReverTra Ace qPCR-RT Master Mix with gDNA Remover (TOYOBO, Osaka, Japan) according to the manufacturer's instructions. RT-qPCR was performed using the AceQ qPCR SYBR Green Master Mix (Vazyme, Nanjing, China) on the Quant Studio 6 Flex Real-Time PCR System (Applied Biosystems, Waltham, MA, USA) according to the manufacturer's instructions. Relative expression level of each sample was determined by normalizing it to the amount of *OsActin1* (LOC_Os03g50885) detected in the same sample and presented as $2^{-\Delta CT}$. All primers used for RT-qPCR are listed in Supplemental Table S2.

Vector construction for mutation or tissue localization of *PHT1;7* in plants and generation of transgenic plants

For gene mutation via the CRISPR–Cas9 system, three different gene-specific spacers (Supplemental Table S1) residing in the open reading frame (ORF) of *PHT1;7* were selected from the rice gene-specific spacers library provided by Miao et al. (2013). These spacers were subcloned into the final expression vector pH-Ubi-cas9-7 as described in Chang et al. (2019). For tissue localization analysis, the expression cassette of *PHT1;7pro::GUSPlus::NOS terminator* was subcloned into the vector pCAMBIA1300. A 2,313-bp DNA fragment upstream of the translation start codon of *PHT1;7* was amplified (primers listed in Supplemental Table S3) from the rice Nipponbare genomic DNA and fused upstream of the GUSPlus reporter gene via *Sal* I/*Hin*d III. The above constructs were transformed into *Agrobacterium* strains EHA105 by electroporation and then transformed into callus derived from mature embryo of Nipponbare developed from the seeds of WT rice plants (cultivar Nipponbare) via *Agrobacterium tumefaciens*-mediated transformation as described in Jia et al. (2011).

GUS staining and immunostaining analysis

The *PHT1;7pro:GUS* transgenic lines were used for histochemical analysis. The GUS staining analysis was performed as described in Ai et al. (2009). Immunostaining analysis with an antibody against GUS was performed as described in Yamaji and Ma (2007), and sections were observed and photographed by a confocal laser scanning microscope (Leica, Wetzlar, Germany; TCS SP8X). The cell wall autofluorescence was excited by ultraviolet light with an intensity of 0.7%–3%; the collection bandwidth and gain value were 410–470 nm and 30%–60%, respectively. The collection bandwidth for Alexa Fluor 555 (the secondary antibody) was 560–580 nm, and the gain value was 50%–60%.

Subcellular localization analysis

For the constructs of subcellular localization, the CDS of *PHT1;7* was subcloned into the pSAT6A-EGFP-N1 vector to generate PHT1;7-GFP. The PHT1;7-GFP as well as alone GFP constructs were transformed into the rice protoplasts by the polyethylene-glycol-mediated method. The isolation and transformation of rice protoplast was performed as described in Jia et al. (2011). OsRac1-mCherry was used as a plasma membrane control. After incubation at 28°C dark for 12–15 h, fluorescence signals in rice protoplasts were observed and photographed by a confocal laser scanning microscope (Leica; TCS SP8X). Excitation/emission wavelengths were 488 nm/498–540 nm for eGFP, 552 nm/600–640 nm for mCherry, and 488 nm/710–760 nm for chloroplast (Chl).

Functional complementation assay of PHT1;7 in yeast or *X. laevis* oocytes

Full-length CDSs of *PHT1;7* and *PHT1;8* were subcloned into the yeast expression vector pAG426GPD-ccdB, and then *PHT1;7*, *PHT1;8* constructs as well as EV were transformed into the yeast mutant strain EY917 defective in Pi uptake (Wykoff and O'Shea, 2001) to check Pi transport activity as described in Chang et al. (2019).

The full-length CDS of *PHT1;7* was subcloned into oocyte expression vector pT7Ts via Bgl II/Spe I. The capped RNA of *PHT1;7* was in vitro transcriptionally synthesized and then injected into oocytes isolated from *X. laevis* as described in Chang et al. (2019). The injected oocytes were incubated at 18°C in Modified Barth's Saline (MBS) solution without NaH_2PO_4 for 48 h before Pi transport assay. The MBS solution contained 88-mM NaCl, 1-mM KCl, 2.4-mM $NaHCO_3$, 0.3-mM Ca $(NO3)2$, 0.41-mM $CaCl_2$, 0.82-mM MgSO4, 15-mM HEPES, and 10-µg/mL sodium penicillin and streptomycin sulfate, adjusted to pH 7.4 using 1-M NaOH. For Pi transport assay, the incubated oocytes were transferred into MBS solution (pH 5.5 or 7.4) supplied with 0.5 mM Pi labeled with ^{32}P orthophosphate (0.5 µCi/µM Pi) for 3 h. After then, the oocytes were washed by cold MBS solution 5 times and every three oocytes were collected in a 5-mL centrifuge tube as one replicate. Oocytes in tubes were digested by a 200 µL mixture (72% $HClO_4$: 30% H_2O_2 = 5:2, by volume) in a 65°C oven for 3 h. Whereafter, 3 mL scintillation cocktail (ULTIMA GOLD LLT; PerkinElmer, Waltham, MA, USA) was added to each tube. ^{32}P radioactivity of each replicate was determined using the liquid scintillation counter (Beckman Coulter, Brea, CA, USA; LS6500).

Measurement of inorganic Pi and total P concentration in plants

For the measurement of inorganic Pi concentration in the plants, fresh samples were weighted and frozen with liquid nitrogen. Frozen samples were handled with the method described by Chang et al. (2019) and finally the absorbance was measured at 820-nm wavelength using a microplate reader (PE, Ensight). Pi concentration of samples was calculated according to measured absorbance and fresh weight.

For the measurement of total P concentration in the plants, samples were dried at 80°C for 3 d to determine the dry weight (DW). For each sample, about 0.05 g dry ground powder was weighted and digested with 3-mL HNO_3 at 180°C. Digested liquid was diluted with ddH_2O, filtered with filter membranes, and measured using an ICP-MS machine (Thermo Fisher Scientific, Waltham, MA, USA; iCAP Q). Total P concentration of samples was calculated according to measured data and DW.

Pollen viability assay

Anthers were collected from five spikelets per tiller one day before anthesis and stained in 2% (w/v) I_2–KI solution. Five tillers at anthesis stage of individual plants of *pht1;7* mutants and the WT were examined. Pollen grains were placed on a glass slide by using forceps to broken anthers. Stained pollen grains were observed and counted by a microscope under bright field. Pollen viability was categorized into three groups: fertile with fully stained (black), partially stained (brown), and not stained (transparent). Three glass slides of each line and five fields of view of each glass slide were observed. In each field of view, no less than 100 pollen grains should be existed.

In vitro and *in vivo* pollen germination assay

Plant materials were grown in a paddy field. For the in vitro pollen germination assay, mature pollen grains collected from *pht1;7* mutants and the WT were germinated in a pollen germination medium, which contained 1-mM $CaCl_2$, 1-mM KCl, 0.8-mM $MgSO_4$, 1.6-mM H_3BO_3, 30-mM $CaSO_4$, 0.03% casein, 0.3% MES, 10% sucrose, and 12.5% polyethylene glycol, on glass slides. The glass slides were incubated at 30°C with >90% relative humidity in a dark box for 2 h, observed and photographed by a microscope under bright field. Three biological replicates were analyzed. Each independent plant was used as one biological replicate, and 5–10 spikelets from each plant were examined. For the in vivo pollen germination assay, the spikelets of *pht1;7* mutants and the WT were collected 2 h after anthesis and fixed in FAA solution (70% ethanol: formalin: acetic acid = 18:1:1, by volume) for 24 h. The samples were washed with an ethanol series (70%, 50%, and 30%) and distilled water, and then incubated in 10 M NaOH for 5–8 min at 56°C. After washing with distilled water 3 times, the spikelets were stained with 0.1% (w/v) aniline blue overnight. Finally, the samples were observed using a fluorescence microscope.

Phylogenetic analysis

The unrooted phylogenetic tree of the rice and Arabidopsis PHT1 homologs was constructed using their amino acid sequences by the Neighbor-Joining algorithm within the MEGA X software. The reference numbers of the protein sequences used for constructing the tree are the following: OsPHT1;1, XP_015631295.1; OsPHT1;2, XP_015630484.1; OsPHT1;3, XP_015614123.1; OsPHT1;4, XP_015636813.1; OsPHT1;5, XP_015635984.1; OsPHT1;6, XP_015649112.1; OsPHT1;7, XP_015630742.1; OsPHT1;8, XP_015614122.1; OsPHT1;9, XP_015642649.1; OsPHT1;10, XP_015642566.1; OsPHT1;11, XP_015633355.1; OsPHT1;12, XP_015631296.1; OsPHT1;13, XP_015634468.1; AtPHT1;1, NP_199149.1; AtPHT1;2, NP_001190462.1; AtPHT1;3, NP_199150.1; AtPHT1;4, NP_181428.1; AtPHT1;5, NP_180842.1; AtPHT1;6, NP_199148.1; AtPHT1;7, NP_001319749.1; AtPHT1;8, NP_173510.1 and AtPHT1;9, NP_177769.1.

Statistical analysis

All the data collected were analyzed for significant differences using the IBM SPSS Statistics version 23 software. Statistical analyses were performed by Duncan's test of one-way analysis of variance. Significance of differences was defined as asterisks ($*P < 0.05$; $**P < 0.01$; $***P < 0.001$) or by different letters ($P < 0.05$).

Accession numbers

Sequence data from this article can be found in the Rice Genome Initiative under the accession numbers in Supplemental Table S2.

Supplemental data

The following materials are available in the online version of this article.

Supplemental Figure S1. Spatio-temporal expression pattern of *PHT1;7* from the RiceXPro database.

Supplemental Figure S2. Expression pattern of *PHT1;7* in spikelets or seeds at different developmental stages from anthesis onward.

Supplemental Figure S3. Subcellular localization of PHT1;7 in rice protoplast.

Supplemental Figure S4. Histochemical staining for GUS activity in transgenic rice plants harboring *ProPHT1;7:GUS* fusion construct.

Supplemental Figure S5. Identification of *ospht1;7* mutant lines.

Supplemental Figure S6. Expression pattern of rice *PHT1* genes in the root of the WT and *pht1;7* mutants at the seedling stage.

Supplemental Figure S7. P concentration (A) and P distribution ratio (B) of different tissues of WT and *pht1;7* mutants at the mature-grain stage.

Supplemental Figure S8. P concentration (A) and P distribution ratio (B) of different tissues of WT and *pht1;7* mutants at anthesis stage.

Supplemental Figure S9. Expression pattern of *OsPHT1;1* and *OsPHT1;6* in anthers of the WT and *pht1;7* mutants.

Acknowledgments

Funding

References

Ai PH, Sun SB, Zhao JN, Fan XR, Xin WJ, Guo Q, Yu L, Shen QR, Wu P, Miller AJ, et al. (2009) Two rice phosphate transporters, OsPht1;2 and OsPht1;6, have different functions and kinetic properties in uptake and translocation. Plant J **57**: 798–809

Ayadi A, David P, Arrighi JF, Chiarenza S, Thibaud MC, Nussaume L, Marin E (2015) Reducing the genetic redundancy of Arabidopsis PHOSPHATE TRANSPORTER1 transporters to study phosphate uptake and signaling. Plant Physiol **167**: 1511–1526

Bayle V, Arrighi JF, Creff A, Nespoulous C, Vialaret J, Rossignol M, Gonzalez E, Paz-Ares J, Nussaume L (2011) *Arabidopsis thaliana* high-affinity phosphate transporters exhibit multiple levels of posttranslational regulation. Plant Cell **23**: 1523–1535

Chang MX, Gu M, Xia YW, Dai XL, Dai CR, Zhang J, Wang SC, Qu HY, Yamaji N, Ma JF, et al. (2019) OsPHT1;3 mediates uptake, translocation, and remobilization of phosphate under extremely low phosphate regimes. Plant Physiol **179**: 656–670

Che J, Yamaji N, Miyaji T, Mitani-Ueno N, Kato Y, Shen RF, Ma JF (2020) Node-localized transporters of phosphorus essential for seed development in rice. Plant Cell Physiol **61**: 1387–1398

Chen LQ, Qu XQ, Hou BH, Sosso D, Osorio S, Fernie AR, Frommer WB (2012) Sucrose efflux mediated by SWEET proteins as a key step for phloem transport. Science **335**: 207–211

Chen LY, Liao H (2017) Engineering crop nutrient efficiency for sustainable agriculture. J Integr Plant Biol **59**: 710–735

Chonan N, Kaneko M, Kawahara H, Matsuda T (1981) Ultrastructure of the large vascular bundles in the leaves of rice plant. JPN J Crop Sci **50**: 323–331

Cong WF, Suriyagoda LD, Lambers H (2020) Tightening the phosphorus cycle through phosphorus-efficient crop genotypes. Trends Plant Sci **25**: 967–975

Conn S, Gilliham M (2010) Comparative physiology of elemental distributions in plants. Ann Bot-Lond **105**: 1081–1102

Fan SC, Lin CS, Hsu PK, Lin SH, Tsay YF (2009) The Arabidopsis nitrate transporter NRT1.7, expressed in phloem, is responsible for source-to-sink remobilization of nitrate. Plant Cell **21**: 2750–2761

Gu M, Chen AQ, Sun SB, Xu GH (2016) Complex regulation of plant phosphate transporters and the gap between molecular mechanisms and practical application: what is missing? Mol Plant **9**: 396–416

Gu M, Hu X, Wang TT, Xu GH (2021) Modulation of plant root traits by nitrogen and phosphate: transporters, long-distance signaling proteins and peptides, and potential artificial traps. Breeding Sci **71**: 62–75

Hammond JP, Broadley MR, White PJ, King GJ, Bowen HC, Hayden R, Meacham MC, Mead A, Overs T, Spracklen WP, et al. (2009) Shoot yield drives phosphorus use efficiency in Brassica oleracea and correlates with root architecture traits. J Exp Bot **60**: 1953–1968

Jia HF, Ren HY, Gu M, Zhao JN, Sun SB, Zhang X, Chen JY, Wu P, Xu GH (2011) The phosphate transporter gene *OsPht1;8* is involved in phosphate homeostasis in rice. Plant Physiol **156**: 1164–1175

Lambers H, Plaxton WC (2015) Phosphorus: back to the roots. Ann Plant Rev **48**: 3–22

Lee SK, Eom JS., Hwang SK, Shin DJ, An G, Okita TW, Jeon JS (2016) Plastidic phosphoglucomutase and ADP-glucose pyrophosphorylase mutants impair starch synthesis in rice pollen grains and cause male sterility. J Exp Bot **67**: 5557–5569

Leegood RC (2008) Roles of the bundle sheath cells in leaves of C3 plants. J Exp Bot **59**: 1663–1673

Lin H, Yu J, Pearce SP, Zhang DB, Wilson ZA (2017) RiceAnternet: a gene co-expression network for identifying anther and pollen development genes. Plant J **92**: 1076–1091

Liu D (2021) Root development responses to phosphorus nutrition. J Integr Plant Biol **63**: 1065–1090

Liu JL, Yang L, Luan MD, Wang Y, Zhang C., Zhang B, Shi J, Zhao FG, Lan WZ, Luan S (2015) A vacuolar phosphate transporter essential for phosphate homeostasis in *Arabidopsis*. Proc Natl Acad Sci USA **112**: E6571–E6578

Liu TY, Huang TK, Yang SY, Hong YT, Huang SM, Wang FN, Chiang SF, Tsai SY, Lu WC, Chiou TJ (2016) Identification of plant vacuolar transporters mediating phosphate storage. Nat Commun **7**: 1–11

Ma B, Zhang L, Gao QF, Wang JM, Li XY, Wang H, Liu Y, Lin H, Liu JY, Wang X, et al. (2021) A plasma membrane transporter coordinates phosphate reallocation and grain filling in cereals. Nat Genet **53**: 906–915

Meng Q, Zhang WQ, Hu X, Shi XY, Chen LL, Dai XL, Qu HY, Xia YW, Liu W, Gu M, et al. (2020) Two ADP-glucose pyrophosphorylase subunits, OsAGPL1 and OsAGPS1, modulate phosphorus homeostasis in rice. Plant J **104**: 1269–1284

Miao J, Guo D, Zhang J, Huang Q, Qin G, Zhang X, Wan J, Gu H, Qu LJ (2013) Targeted mutagenesis in rice using CRISPR-Cas system. Cell Res **23**: 1233–1236

Mudge SR, Rae AL, Diatloff E, Smith FW (2002) Expression analysis suggests novel roles for members of the Pht1 family of phosphate transporters in *Arabidopsis*. Plant J **31**: 341–353

Nagarajan VK, Jain A, Poling MD, Lewis AJ, Raghothama KG, Smith AP (2011) Arabidopsis Pht1;5 mobilizes phosphate between source and sink organs and influences the interaction between phosphate homeostasis and ethylene signaling. Plant Physiol 156: 1149–1163

Oelkers EH, Valsami-Jones E (2008) Phosphate mineral reactivity and global sustainability. Elements 4: 83–87

Ono E, Wong HL, Kawasaki T, Hasegawa M, Kodama O, Shimamoto K (2001) Essential role of the small GTPase Rac in disease resistance of rice. Proc Natl Acad Sci USA 98: 759–764.

Preuss CP, Huang CY, Gilliham M, Tyerman SD (2010) Channel-like characteristics of the low-affinity barley phosphate transporter PHT1;6 when expressed in Xenopus oocytes. Plant Physiol 152: 1431–1441

Rae AL, Cybinski DH, Jarmey JM, Smith FW (2003) Characterization of two phosphate transporters from barley; evidence for diverse function and kinetic properties among members of the Pht1 family. Plant Mol Biol 53: 27–36

Raghothama KG (1999) Phosphate acquisition. Annu Rev Plant Phys 50: 665–693

Regmi KC, Zhang SJ, Gaxiola RA (2016) Apoplasmic loading in the rice phloem supported by the presence of sucrose synthase and plasma membrane-localized proton pyrophosphatase. Ann Bot-Lond 117: 257–268

Remy E, Cabrito TR, Batista RA, Teixeira MC, Sá-Correia, I, Duque P (2012) The Pht1;9 and Pht1;8 transporters mediate inorganic phosphate acquisition by the Arabidopsis thaliana root during phosphorus starvation. New Phytol 195: 356–371

Sage TL, Sage RF (2009) The functional anatomy of rice leaves: implications for refixation of photorespiratory CO$_2$ and efforts to engineer C4 photosynthesis into rice. Plant Cell Physiol 50: 756–772

Santiago JP, Tegeder M (2016) Connecting source with sink: the role of Arabidopsis AAP8 in phloem loading of amino acids. Plant Physiol 171: 508–521

Sato Y, Takehisa H, Kamatsuki K, Minami H, Namiki N, Ikawa H, Ohyanagi H, Sugimoto K, Antonio B, Nagamura Y (2013) RiceXPro Version 3.0: expanding the informatics resource for rice transcriptome. Nucleic Acids Res 41: D1206–D1213

Schroeder JI, Delhaize E, Frommer WB, Guerinot ML, Harrison MJ, Herrera-Estrella L, Horie T, Kochian LV, Munns R, Nishizawa NK, et al. (2013) Using membrane transporters to improve crops for sustainable food production. Nature 497: 60–66

Shatil-Cohen A, Moshelion M (2012) Smart pipes: the bundle sheath role as xylem-mesophyll barrier. Plant Signal Behav 7: 1088–1091

Shin H, Shin HS, Dewbre GR, Harrison MJ (2004) Phosphate transport in Arabidopsis: pht1;1 and Pht1;4 play a major role in phosphate acquisition from both low- and high-phosphate environments. Plant J 39: 629–642

Stadler R, Sauer N (1996) The Arabidopsis thaliana AtSUC2 gene is specifically expressed in companion cells. Bot Acta 109: 299–306

Sun SB, Gu M, Cao Y, Huang XP, Zhang X, Ai PH, Zhao JN, Fan XR, Xu GH (2012) A constitutive expressed phosphate transporter, OsPht1;1, modulates phosphate uptake and translocation in phosphate-replete rice. Plant Physiol 159: 1571–1581

Ueno D, Sasaki A, Yamaji N, Miyaji T, Fujii Y, Takemoto Y, Moriyama S, Che J, Moriyama Y, Iwasaki K, et al. (2015) A polarly localized transporter for efficient manganese uptake in rice. Nat Plants 1: 15170

Van Kauwenbergh SJ (2010) World Phosphate Rock Reserves and Resources, Technical Bulletin International Fertilizer Development Center (IFDC)-T-75, Muscle Shoals, AL, USA

Veneklaas EJ, Lambers H, Bragg J, Finnegan PM, Lovelock CE, Plaxton WC, Price CA, Scheible WR, Shame MW, White PJ, et al. (2012) Opportunities for improving phosphorus-use efficiency in crop plants. New Phytol 195: 306–320

Wang C, Huang W, Ying YH, Li S, Secco D, Tyerman S, Whelan J, Shou HX (2012) Functional characterization of the rice SPX-MFS family reveals a key role of OsSPX-MFS1 in controlling phosphate homeostasis in leaves. New Phytol 196: 139–148

Wang C, Yue WH, Ying YH, Wang SD, Secco D, Liu Y, Whelan J, Tyerman SD, Shou HX (2015) Rice SPX-Major Facility Superfamily3, a vacuolar phosphate efflux transporter, is involved in maintaining phosphate homeostasis in rice. Plant Physiol 169: 2822–2831

Wang FM, Rose T, Jeong K, Kretzschmar T, Wissuwa M (2016) The knowns and unknowns of phosphorus loading into grains, and implications for phosphorus efficiency in cropping systems. J Exp Bot 67: 1221–1229

Wang GP, Wu Y, Ma L, Lin Y, Hu YX, Li MZ, Li WW, Ding YF, Chen L (2021d). Phloem loading in rice leaves depends strongly on the apoplastic pathway. J Exp Bot 72: 3723–3738

Wang JX, Pan WB, Nikiforov A, King W, Hong WT, Li WW, Han Y, Patton-Vogt J, Shen JB, Cheng LY (2020) Identification of two glycerophosphodiester phosphodiesterase genes in maize leaf phosphorus remobilization. Crop J 9: 95–108

Wang L, Jia XQ, Zhang YX, Xu L, Menand B, Zhao HY, Zeng HQ, Dolan L, Zhu YY, Yi KK (2021c) Loss of two families of SPX domain-containing proteins required for vacuolar polyphosphate accumulation coincides with the transition to phosphate storage in green plants. Mol Plant 14: 838–846

Wang W, Ding GD, White PJ, Wang XH, Jin KM, Xu FS, Shi L (2019) Mapping and cloning of quantitative trait loci for phosphorus efficiency in crops: opportunities and challenges. Plant Soil 439: 91–112

Wang XF, Wang YF, Piñeros MA, Wang ZY, Wang WX, Li CY, Wu ZC, Kochian LV, Wu P (2014) Phosphate transporters OsPHT1;9 and OsPHT1;10 are involved in phosphate uptake in rice. Plant Cell Environ 37: 1159–1170

Wang Y, Chen YF, Wu WH (2021b) Potassium and phosphorus transport and signaling in plants. J Integr Plant Biol 63: 34–52

Wang Y, Wang F, Lu H, Liu Y, Mao C (2021a) Phosphate uptake and transport in plants: an elaborate regulatory system. Plant Cell Physiol 62: 564–572

Wigoda N, Moshelion M, Moran N (2014) Is the leaf bundle sheath a "smart flux valve" for K$^+$ nutrition? J Plant Physiol 171: 715–722

Wykoff DD, O'Shea EK (2001) Phosphate transport and sensing in saccharomyces cerevisiae. Genetics 159: 1491–1499

Xu L, Zhao HY, Wan RJ, Liu Y, Xu Z, Tian W, Ruan WY, Wang F, Deng MJ, Wang JM, et al. (2019) Identification of vacuolar phosphate efflux transporters in land plants. Nat Plants 5: 84–94

Yamada N (1972) Studies on the developmental physiology in rice pollen: I. The metabolic patterns connected with the structural changes in developing pollen. JPN J Crop Sci 41: 320–334

Yamaji N, Ma JF (2007) Spatial distribution and temporal variation of the rice silicon transporter Lsi1. Plant Physiol 143: 1306–1313

Yamaji N, Ma JF (2014) The node, a hub for mineral nutrient distribution in graminaceous plants. Trends Plant Sci 19: 556–563

Yamaji N, Ma JF (2017) Node-controlled allocation of mineral elements in Poaceae. Curr Opin Plant Biol 39: 18–24

Yamaji N, Takemoto Y, Miyaji T, Mitani-Ueno N, Yoshida KT, Ma JF (2017) Reducing phosphorus accumulation in rice grains with an impaired transporter in the node. Nature 541: 92–95

Yamaji N, Xia J, Mitani-Ueno N, Yokosho K, Ma JF (2013) Preferential delivery of zinc to developing tissues in rice is mediated by P-type heavy metal ATPase OsHMA2. Plant Physiol 162: 927–939

Yang SY, Lu WC, Ko SS, Sun CM., Hung JC, Chiou TJ (2020) Upstream open reading frame and phosphate-regulated expression of rice OsNLA1 controls phosphate transport and reproduction. Plant Physiol 182: 393–407

Ye Y, Yuan J, Chang XJ, Yang M, Zhang LJ, Lu K, Lian XM (2015) The phosphate transporter gene OsPht1;4 is involved in phosphate homeostasis in rice. PLoS One 10: e0126186

Yue WH, Ying YH, Wang C, Zhao Y, Dong CH, Whelan J, Shou HX (2017) OsNLA1, a RING-type ubiquitin ligase, maintains phosphate homeostasis in *Oryza sativa* via degradation of phosphate transporters. Plant J **90**: 1040–1051

Zhang C, Turgeon R (2018) Mechanisms of phloem loading. Curr Opin Plant Biol **43**: 71–75

Zhang F, Sun YF, Pei WX, Jain A, Sun R, Cao Y, Wu XN, Jiang TT, Zhang L, Fan XR, et al. (2015) Involvement of OsPHT1;4 in phosphate acquisition and mobilization facilitates embryo development in rice. Plant J **82**:556–569

Zhang J, Gu M, Liang RSH, Shi XY, Chen LL, Hu X, Wang SC, Dai XL, Qu HY, Li HH, Xu GH (2021) OsWRKY21 and OsWRKY108 function redundantly to promote phosphate accumulation through maintaining the constitutive expression of OsPHT1;1 under phosphate-replete conditions. New Phytol **229**: 1598–161